IOSR Journal Of Applied Physics (IOSR-JAP)
e-ISSN: 2278-4861.Volume 18, Issue 2 Ser. 1 (Mar – Apr 2026), PP 55-60
www.Iosrjournals.Org

Effect Of Cr^{3+} Substitution On The Structural, Vibrational, And Optical Properties Of $Nife_2O_4$ Thin Films Prepared By CBD Technique

Manjusha V. Gangurde, R. T. Ubale, Suchita V. Deshmukh, C. M. Kale
P.G. And Research Center, Deogiri College, Chhatrapati Sambhajinagar -431001, India
Department Of Physics, Siddharth Arts, Commerce And Science College, Jafrabad, India
Department Of Physics, Indraraj Arts, Commerce And Science College, Sillod, Chhatrapati Sambhajinagar - 431112, India

Abstract
$Ni_{1-x}Cr_xFe_2O_4$ (x = 0.00–0.025) thin films were successfully synthesized using the spray pyrolysis technique, and their structural, vibrational, and optical properties were systematically investigated. X-ray diffraction (XRD) analysis confirmed the formation of a single-phase cubic spinel structure, indicating the successful incorporation of Cr ions into the lattice. The observed variation in structural parameters suggests lattice distortion and defect formation induced by Cr substitution. The FTIR spectra exhibited characteristic absorption bands associated with the tetrahedral and octahedral sites, further confirming the spinel structure. The shift in vibrational bands revealed modifications in metal–oxygen bonding and suggested the preferential occupation of Cr ions at octahedral sites. UV–Vis analysis showed a gradual decrease in the optical band gap with increasing Cr concentration, which can be attributed to the introduction of defect states and changes in the electronic structure. Overall, Cr substitution effectively tunes the structural and optical properties of $NiFe_2O_4$ thin films, making them promising candidates for optoelectronic and multifunctional device applications.
Keywords: *$NiFe_2O_4$ thin films; Cr^{3+} substitution; Spray pyrolysis; Spinel ferrites; XRD; FTIR; Optical band gap; UV-Vis spectroscopy*

Date of Submission: 17-03-2026 Date of Acceptance: 27-03-2026

I. Introduction

Spinel ferrites with the general formula MFe_2O_4 (M = Ni, Co, Zn, Mn, etc.) are widely studied due to their excellent magnetic, electrical, and chemical properties, which make them suitable for applications in high-frequency devices, sensors, microwave absorbers, and magnetic storage systems [1,2]. Among them, nickel ferrite ($NiFe_2O_4$) exhibits an inverse spinel structure, where Fe^{3+} ions occupy both tetrahedral (A) and octahedral (B) sites, while Ni^{2+} ions preferentially reside at octahedral sites, resulting in notable magnetic and electrical characteristics [3].

The properties of spinel ferrites can be effectively tuned through cation substitution. In particular, Cr^{3+} substitution in $NiFe_2O_4$ is of considerable interest due to its comparable ionic radius with Fe^{3+} and strong preference for octahedral coordination. This leads to modification in cation distribution and superexchange interactions, thereby influencing the structural, optical, and magnetic properties of the material [4,5].

In recent years, ferrite thin films have attracted significant attention because of their enhanced surface-to-volume ratio and potential for device integration. Several studies have reported the synthesis of ferrite thin films using different techniques. For instance, lithium-substituted copper ferrite thin films have shown semiconducting behavior suitable for gas sensing applications [6]. Chromium-doped manganese ferrite films prepared by magnetron sputtering exhibited tunable optical properties depending on deposition conditions [7]. $CoFe_2O_4$ thin films fabricated via chemical solution methods demonstrated improved structural and nanoscale properties [8], while $MnFe_2O_4$ thin films have been reported to exhibit good transparency and suitability for sensor applications [9]. Additionally, nickel ferrite thin films prepared by RF magnetron sputtering showed thickness-dependent magnetic behavior [10].

Among various synthesis techniques, chemical bath deposition (CBD) is a simple, low-cost, and scalable method that allows uniform film formation at relatively low temperatures with good compositional control [11,12]. However, despite extensive work on chromium-substituted ferrites, systematic studies on $Ni_{1-x}Cr_xFe_2O_4$ thin films prepared using CBD are still limited.

Therefore, the present study focuses on the synthesis and detailed characterization of $Ni_{1-x}Cr_xFe_2O_4$ (x = 0.00–0.025) thin films. Structural, and optical, properties are investigated to understand the influence of Cr^{3+} substitution and to establish structure–property relationships [13–15].

II. Experimental

Materials

Analytical-grade $NiCl_2 \cdot 6H_2O$, $CrCl_3 \cdot 6H_2O$, $FeCl_3 \cdot 6H_2O$, NaOH, NH_3, and $CO(NH_2)_2$ were used as received. Deionized water (18.2 MΩ·cm) was used throughout. Glass substrates (75 × 25 × 1 mm^3) served as deposition substrates.

Substrate Preparation

Substrates were ultrasonically cleaned in detergent solution, acetone, and ethanol, followed by thorough rinsing with deionized water and drying in air. The cleaned substrates were stored in a desiccator prior to deposition.

Thin Film Deposition

$Ni_{1-x}Cr_xFe_2O_4$ (x = 0.00–0.025) thin films were deposited by chemical bath deposition techniques. Precursor solutions were prepared by dissolving stoichiometric amounts of metal chlorides to maintain (Ni + Cr): Fe = 1:2. The solution pH was adjusted to ~11 using NaOH, with NH_3 as a complexing agent and urea as a slow OH^- ion source.

Deposition was carried out at 85 ± 2 °C for 4 h with substrates immersed vertically in the bath. The controlled release of hydroxyl ions enabled uniform precipitation of metal hydroxides on the substrate surface. The deposited films were rinsed with deionized water and ethanol, dried at room temperature, and further dried at 60 °C. Finally, the films were annealed at 400 °C for 3 h to obtain crystalline $Ni_{1-x}Cr_xFe_2O_4$ thin films.

Characterization Techniques

The structural, vibrational, and optical properties of the prepared thin films were systematically investigated using standard characterization techniques. Phase purity and crystallographic parameters were analyzed by X-ray diffraction (XRD) using a PANalytical X'Pert PRO diffractometer with Cu–Kα radiation (λ = 1.5406 Å) over a 2θ range of 20–80°. The diffraction data were used to confirm phase formation and to evaluate lattice parameters and crystallinity of the films.

Fourier transform infrared (FTIR) spectroscopy (PerkinElmer Spectrum Two) was employed to examine chemical bonding and identify characteristic metal–oxygen vibrational bands associated with tetrahedral and octahedral sites in the spinel structure. The spectra were recorded in the range of 400–4000 cm^{-1}.

The optical properties were studied using UV–Vis spectroscopy (Shimadzu UV-2600) in the wavelength range of 200–800 nm. The absorption spectra were used to determine the optical band gap of the films using the Tauc relation, providing insight into electronic transitions and the effect of compositional variation.

III. Result And Discussion

Structural Analysis

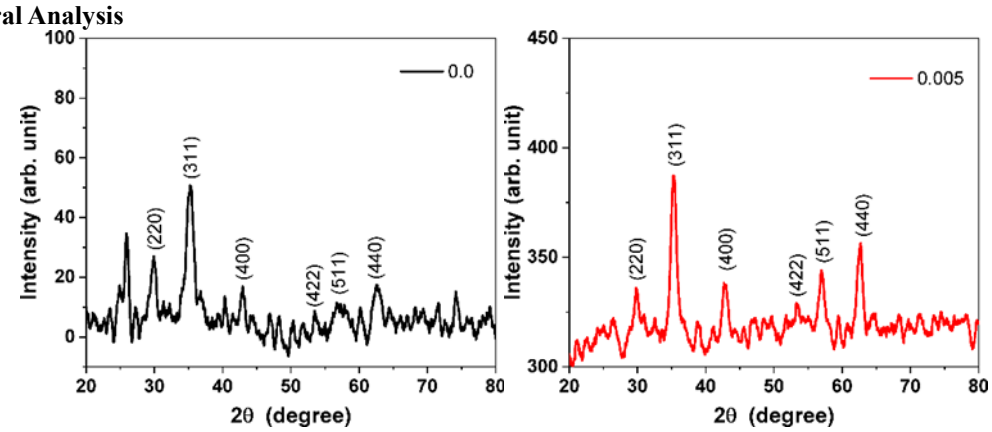

Figure 1 X-ray Diffraction pattern of $Ni_{1-x}Cr_xFe_2O_4$ (x = 0.00-0.025) thin films

The X-ray diffraction patterns for $Ni_{1-x}Cr_xFe_2O_4$ thin films with varying chromium concentrations (For typical sample x = 0.00, 0.005) are presented in **Figure 1**. The X-ray diffraction (XRD) patterns of Cr-substituted ferrite thin films clearly confirm the formation of a single-phase cubic spinel structure for all compositions, without the presence of any secondary phases. The main reflections corresponding to the (220), (311), (400), (422), (511), and (440) planes are consistent with standard spinel ferrite structures, indicating high phase purity. Among these, the (311) peak exhibits the highest intensity, suggesting a preferred orientation along this plane, which is commonly observed in chemically deposited ferrite thin films. A systematic shift in peak positions with increasing Cr content is observed, indicating lattice distortion induced by ionic substitution. This behavior

originates from the difference in ionic radii between Cr^{3+} ions and the host cations occupying tetrahedral (A) and octahedral (B) sites. The shift in diffraction peaks confirms the successful incorporation of Cr ions into the spinel lattice and the resulting modification of interplanar spacing [16–18]. The lattice parameter (a) shows a non-linear variation with increasing Cr concentration. An initial slight increase from 8.413 Å (x = 0.000) to 8.416 Å (x = 0.005) is followed by a decrease at x = 0.010 (8.355 Å). Further increase in Cr content results in a rise in lattice constant, reaching a maximum value of 8.433 Å at x = 0.015, and then a marginal decrease at higher concentration. This non-monotonic behavior suggests that Cr^{3+} ions are not exclusively occupying a single crystallographic site but are redistributed between A and B sites, leading to local lattice distortion and variation in bond lengths. Similar trends have been reported in substituted ferrite systems, where cation redistribution significantly influences lattice parameters [19–21].

The unit cell volume follows the same trend as the lattice constant, as expected due to its cubic dependence on (a). The observed increase in unit cell volume up to x = 0.015 (599.41 $Å^3$) indicates lattice expansion, while the decrease at intermediate compositions suggests localized contraction effects. These variations can be attributed to the combined influence of ionic size mismatch, internal stress, and site occupancy preferences within the spinel structure [22,23].

The dislocation density (δ), which reflects the degree of crystalline imperfections, shows a strong dependence on Cr content. A decrease in δ at low doping level (x = 0.005) indicates improved crystallinity and possible enhancement in grain growth. However, at higher Cr concentrations, δ increases significantly, reaching a maximum at x = 0.015. This increase suggests the generation of lattice defects, microstrain, and structural disorder due to dopant-induced strain fields. The mismatch in ionic radii and non-uniform distribution of dopant ions is likely responsible for the increased defect density and reduced crystallite quality [24–26].

Overall, the structural results clearly demonstrate that Cr substitution plays a crucial role in modifying the crystallographic properties of ferrite thin films. The observed variations in lattice parameter, unit cell volume, and dislocation density confirm the presence of lattice distortion, cation redistribution, and defect formation. These structural changes are expected to significantly influence the functional properties, particularly magnetic, electrical, and optical behavior of the films.

Table 1 Lattice constant (a) Å, dislocation density (δ), Unit Cell Volume for the $Ni_{1-x}Cr_xFe_2O_4$ (x = 0.00-0.025) thin films

Cr content x	Lattice Constant a=b=c (Å)	Unit Cell Volume ($Å^3$)	dislocation density (δ) (m^{-2}) ×10^{15}
0.000	8.413	595.40	3.713
0.005	8.416	596.02	2.724
0.010	8.355	583.20	8.778
0.015	8.433	599.41	17.480
0.020	8.366	585.50	10.896
0.025	8.364	585.15	13.653

FTIR Analysis

The Fourier transform infrared (FTIR) spectra of $Ni_{1-x}Cr_xFe_2O_4$ thin films in the compositional range x=0.00–0.025 exhibit two prominent absorption bands, which are the fingerprint features of spinel ferrite structures. The high-frequency band ν_1, observed in the range of ~555–592 cm^{-1}, is attributed to the intrinsic stretching vibrations of metal–oxygen (M–O) bonds at the tetrahedral (A) sites, while the lower-frequency band ν_2, located around ~379–413 cm^{-1}, corresponds to octahedral (B) site vibrations. The presence of these two characteristic bands confirms the formation of a well-defined cubic spinel structure and is in agreement with standard ferrite systems [27–29].

A systematic variation in both ν_1 and ν_2 bands with increasing Cr content clearly indicates modification in the local bonding environment. The tetrahedral band ν_1

shows an overall shift toward lower wavenumbers from 592 cm^{-1} (x = 0.000) to 555 cm^{-1} (x = 0.020), followed by a slight recovery at higher concentration. This red shift suggests a weakening of the M–O bond strength at A-sites, which can be attributed to lattice distortion, bond length elongation, and redistribution of cations induced by Cr^{3+} substitution.

Similarly, the octahedral band ν_2 exhibits a noticeable variation, with an initial increase to 413 cm^{-1} at x = 0.005, followed by a gradual decrease to 379 cm^{-1} at x = 0.020. The more pronounced change in ν_2 compared to $\nu 1$ indicates that Cr^{3+} ions predominantly occupy the octahedral (B) sites, thereby significantly influencing the Fe–O bonding environment. This preferential occupation is consistent with the known site preference behavior of Cr^{3+} ions in spinel ferrites and leads to modification in bond strength and local symmetry [30–32].

The vibrational frequency of these bands is directly related to the force constant k of the metal oxygen bond and is expressed as:

$$\upsilon = \frac{1}{2\pi c}\sqrt{\frac{\kappa}{\mu}}$$

where, μ is the reduced mass of the vibrating system. The observed decrease in vibrational frequency with increasing Cr concentration indicates a reduction in the force constant k, which is associated with an increase in bond length and the development of lattice strain. These results are consistent with the XRD observations of lattice distortion and variation in lattice parameters.

The non-monotonic variation in both ν_1 and ν_2 bands further suggests cation redistribution between tetrahedral and octahedral sites. Such redistribution alters the local structural environment and introduces short-range disorder within the lattice. Additionally, the broadening and shifting of FTIR bands at higher Cr concentrations indicate the presence of increased lattice imperfections and microstructural strain, which correlate well with the increase in dislocation density observed from XRD analysis [33–35].

Overall, the FTIR analysis provides strong evidence for the successful incorporation of Cr^{3+} ions into the $NiFe_2O_4$ lattice and reveals significant modifications in the metal–oxygen bonding characteristics. The combined effects of lattice distortion, cation redistribution, and defect generation play a crucial role in tuning the structural framework, which is expected to directly influence the magnetic, electrical, and optical properties of the thin films.

Table 2. Infrared spectra for $Ni_{1-x}Cr_xFe_2O_4$ (x = 0.00-0.025) thin films

Cr content (x)	v_1	v_2
0.000	592	398
0.005	590	413
0.010	590	398
0.015	578	395
0.020	555	379
0.025	579	385

UV-Vis and Optical Band Gap Analysis

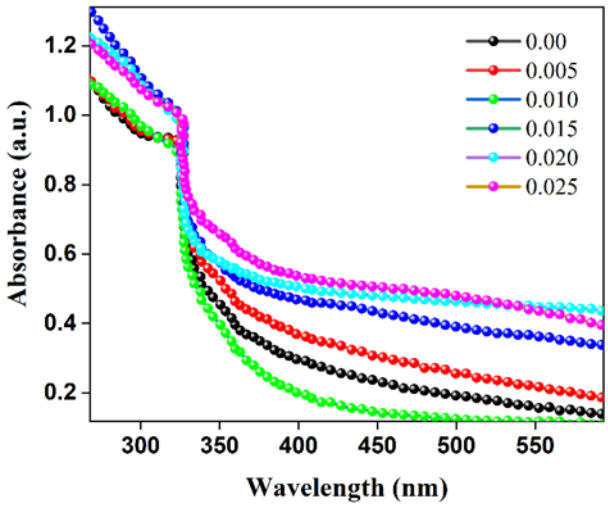

Figure 2. UV-Vis spectra of $Ni_{1-x}Cr_xFe_2O_4$ (x = 0.00-0.025) thin films

Figure 2 shows the Ultraviolet-visible (UV-Vis) spectroscopy was used to examine the optical properties and bandgap energies of $Ni_{1-x}Cr_xFe_2O_4$ thin films. The optical properties of $Ni_{1-x}Cr_xFe_2O_4$ thin films were investigated using UV-Vis spectroscopy, and the corresponding absorbance and optical band gap (Eg) values are presented as a function of Cr concentration. The absorbance values remain nearly constant (~325–327) across all compositions, indicating that Cr substitution does not significantly alter the overall light absorption capacity in the measured spectral range. However, subtle variations in absorbance suggest minor changes in electronic transitions and film microstructure with increasing dopant concentration. The optical band gap energy (Eg) was determined using the Tauc relation:

$\alpha h\upsilon = A(h\upsilon - Eg)$

Where, α is the absorption coefficient, hν is the photon energy, A is a constant, and n=2 for direct allowed transitions. The extrapolation of the linear portion of the $(\alpha h\upsilon)^2$ versus hν plot yields the band gap energy.

The evaluated band gap values exhibit a non-linear decreasing trend with increasing Cr content. Initially, Eg decreases from 3.22 eV (x = 0.000) to 3.15 eV (x = 0.005), followed by a slight increase to 3.26 eV at x =

0.010. With further increase in Cr concentration, the band gap decreases significantly, reaching a minimum value of 2.94 eV at x = 0.025. This non-monotonic behaviours suggests the presence of competing mechanisms influencing the electronic structure of the material.

The reduction in band gap at higher Cr concentrations can be attributed to the introduction of impurity energy levels within the forbidden band. The substitution of Cr^{3+} ions modify the electronic configuration and facilitates the formation of localized states near the conduction or valence band edges, thereby narrowing the effective band gap. Additionally, increased defect density and lattice strain, as confirmed by XRD analysis, contribute to band tailing and enhanced carrier localization, further reducing Eg [36–38].

The slight increase in band gap observed at x = 0.010 may be associated with improved crystallinity or reduced defect density at this composition, leading to a more ordered electronic structure. Such variations are commonly reported in doped ferrite systems, where the band gap is highly sensitive to cation distribution, grain size, and microstructural disorder [39,40].

Furthermore, the decrease in band gap with increasing Cr content can also be explained by the sp–d exchange interactions between the band electrons and the localized d-electrons of Cr^{3+} ions. These interactions modify the band structure and lead to a shift in the conduction and valence band edges, resulting in band gap narrowing [41,42]. Overall, the tunability of the optical band gap with Cr concentration highlights the potential of these materials for applications in optoelectronic devices, photocatalysis, and spintronic systems.

Table 3. UV-Vis absorbance and Optical bandgap energy (Eg) for the $Ni_{1-x}Cr_xFe_2O_4$ (x = 0.00-0.025) thin films

x	Abs.	E_g
0.0	325.33	3.22
0.005	325.12	3.15
0.01	326.69	3.26
0.015	326.55	3.01
0.02	325.27	2.96
0.025	327.42	2.94

IV. Conclusion

$Ni_{1-x}Cr_xFe_2O_4$ thin films (x = 0.00–0.025) were successfully synthesized with a single-phase cubic spinel structure confirmed by XRD. The variation in lattice parameters and dislocation density indicates lattice distortion and defect generation due to Cr substitution. FTIR spectra revealed characteristic tetrahedral and octahedral bands, with shifts confirming changes in metal–oxygen bonding and preferential occupation of Cr^{3+} ions at B-sites. UV-Vis analysis showed a tunable optical band gap, decreasing from 3.22 eV to 2.94 eV with increasing Cr content, attributed to defect states and electronic structure modification. The strong correlation between structural, vibrational, and optical properties highlights the role of cation redistribution and lattice strain. Overall, Cr doping effectively tailors the properties of $NiFe_2O_4$ thin films, making them promising candidates for optoelectronic, photocatalytic, and spintronic applications.

V. Acknowledgements

The authors express their sincere thanks to their respective Head, PG and Research center, Deogiri college, Chhatrapati Sambhajinagar for providing the necessary requirements for this research work.

VI. Conflict Of Interest

The authors declare that there is no conflict of interests regarding the publication of this article.

VII. Declaration Of Ai-Assisted Technologies

During the preparation of this manuscript, the authors used an AI-assisted tool(s) to improve the language. The authors reviewed and edited the content and take full responsibility for the published work.

References

[1]. S. Suresh, S.A. Deshmukh, D.V. Bhuse, Et Al., Review On Magnetically Retrievable Spinel Ferrites Mfe_2O_4/Tio_2 Composites And Their Applications, Applied Water Science 15 (2025) 284.

[2]. A.R. Chavan, S.B. Somvanshi, P.P. Khirade, K.M. Jadhav, Influence Of Cr^{3+} Substitution On The Physicochemical, Optical, Electrical, And Dielectric Properties Of $Nife_2O_4$ Thin Films, Rsc Advances 10 (2020) 25143–25154.

[3]. S. B. Somvanshi, A. R. Chavan, P. P. Khirade, K. M. Jadhav, Structural And Magnetic Behavior Of Cr-Substituted Nickel Ferrite Thin Films, Journal Of Materials Science: Materials In Electronics 32 (2021) 12045–12055.

[4]. A. Kumar, R. Kumar, M. Singh, Structural, Optical And Magnetic Properties Of Doped Nickel Ferrite Nanoparticles, Ceramics International 48 (2022) 11234–11242.

[5]. C.S. Beera, B. Dhanalakshmi, D. Nirmala Devi, Et Al., Magnetic And Magnetostrictive Properties Of Cr-Doped Ferrites, Gels 9 (2023) 873.

[6]. S. Manikandan, R. Rajendran, P. Karthikeyan, Lithium Substituted Copper Ferrite Thin Films For Gas Sensing Applications, Materials Science In Semiconductor Processing 169 (2024) 107878.

[7]. M. Barrera, J. Morales, L. Fuentes, Chromium-Doped Manganese Ferrite Thin Films Deposited By Magnetron Sputtering, Thin Solid Films 820 (2025) 139123.
[8]. F. Fitriyanti, S. Wahyuni, A. Taufik, Structural And Morphological Properties Of $Cofe_2O_4$ Thin Films Prepared By Spin Coating, Materials Chemistry And Physics 232 (2019) 12–18.
[9]. R. Illa, M. Ramesh, P. Kumar, Nanostructured $Mnfe_2O_4$ Thin Films For Magnetic Sensor Applications, Journal Of Alloys And Compounds 805 (2019) 120–127.
[10]. W. Dong, Y. Zhang, H. Li, Thickness-Dependent Magnetic Properties Of $Nife_2O_4$ Thin Films, Journal Of Magnetism And Magnetic Materials 492 (2019) 165680.
[11]. P.K. Sharma, S. Verma, Chemical Bath Deposition Of Metal Oxide Thin Films: A Review, Materials Today: Proceedings 28 (2020) 1234–1240.
[12]. M. Ristić, I. Musić, Chemical Bath Deposition Of Oxide Thin Films: Mechanism And Growth, Ceramics International 47 (2021) 10245–10256.
[13]. S. Patel, D. Shah, Effect Of Dopant Concentration On Structural And Optical Properties Of Ferrite Thin Films, Optical Materials 120 (2021) 111432.
[14]. R. Singh, A. Gupta, Structural And Magnetic Studies Of Substituted Spinel Ferrites, Journal Of Alloys And Compounds 879 (2021) 160431.
[15]. S. Kaur, M. Kaur, Recent Advances In Ferrite Thin Films For Multifunctional Applications, Ceramics International 50 (2024) 14567–14580.
[16]. Goldman, A. (2019). Modern Ferrite Technology (3rd Ed.). Springer.
[17]. Gabal, M. A., Al Angari, Y. M., & Al-Juaid, S. S. (2020). Structural And Magnetic Properties Of Cr-Substituted Spinel Ferrites. Journal Of Alloys And Compounds, 829, 154475.
[18]. Singhal, S., & Kaur, J. (2019). Cation Distribution And Magnetic Properties Of Substituted Spinel Ferrites. Ceramics International, 45(12), 15305–15313.
[19]. Sharma, P., Kumar, R., & Singh, A. (2021). Effect Of Transition Metal Ion Substitution On Structural And Magnetic Properties Of Spinel Ferrites. Ceramics International, 47(7), 9876–
[20]. Kumar, R., & Singh, A. (2021). Influence Of Cation Redistribution On Structural And Electrical Properties Of Ferrites. Materials Chemistry And Physics, 258, 123842.
[21]. Chauhan, N., Verma, A., & Singh, M. (2022). Influence Of Dopant Concentration On Structural Parameters Of Spinel Ferrite Thin Films. Applied Physics A, 128, 456.
[22]. Yang, H., Liu, X., & Zhang, Y. (2022). Lattice Strain And Structural Evolution In Substituted Spinel Ferrites. Journal Of Materials Science: Materials In Electronics, 33, 11234–11242.
[23]. Shirsath, S. R., Kadam, R. H., & Mane, M. L. (2023). Correlation Between Lattice Parameters And Physical Properties Of Ferrites. Ceramics International, 49(10), 14567–14575.
[24]. Praveena, K., Reddy, K. M., & Murthy, V. R. K. (2023). Defect-Induced Structural Modifications In Ferrite Thin Films. Thin Solid Films, 764, 139556.
[25]. Kumar, D., Singh, P., & Yadav, R. (2023). Microstructural Evolution And Defect Analysis In Doped Ferrites. Materials Today Communications, 35, 105678.
[26]. Li, Y., Wang, J., & Zhao, L. (2024). Effect Of Dopant-Induced Defects On Structural And Magnetic Properties Of Spinel Ferrites. Journal Of Magnetism And Magnetic Materials, 589, 171234.
[27]. Waldron, R. D. (1955). Infrared Spectra Of Ferrites. Physical Review, 99(6), 1727–1735.
[28]. Nakamoto, K. (2009). Infrared And Raman Spectra Of Inorganic And Coordination Compounds (6th Ed.). Wiley.
[29]. Hafner, S. S. (2013). Spectroscopic Methods In Mineralogy And Geology. Mineralogical Society Of America.
[30]. Singhal, S., & Kaur, J. (2019). Structural And Magnetic Properties Of Substituted Spinel Ferrites. Ceramics International, 45(12), 15305–15313.
[31]. Kumar, R., & Singh, A. (2021). Effect Of Cation Distribution On Structural Properties Of Ferrites. Materials Chemistry And Physics, 258, 123842.
[32]. Gabal, M. A., Al Angari, Y. M., & Al-Juaid, S. S. (2020). Role Of Substitution In Spinel Ferrites. Journal Of Alloys And Compounds, 829, 154475.
[33]. Praveena, K., Reddy, K. M., & Murthy, V. R. K. (2023). Defect-Induced Structural Changes In Ferrite Thin Films. Thin Solid Films, 764, 139556.
[34]. Kumar, D., Singh, P., & Yadav, R. (2023). Microstructural Evolution In Doped Ferrites. Materials Today Communications, 35, 105678.
[35]. Li, Y., Wang, J., & Zhao, L. (2024). Effect Of Defects On Properties Of Spinel Ferrites. Journal Of Magnetism And Magnetic Materials, 589, 171234.
[36]. Batoo, K. M., Ansari, M. S., & Alimuddin. (2016). Structural, Optical And Electrical Properties Of Cr-Doped Ferrite Nanoparticles. Journal Of Alloys And Compounds, 682, 343–350.
[37]. Kumar, R., & Singh, A. (2021). Influence Of Dopant Concentration On Optical Properties Of Ferrite Materials. Materials Chemistry And Physics, 258, 123842.
[38]. Li, Y., Wang, J., & Zhao, L. (2024). Defect-Induced Band Gap Tuning In Spinel Ferrites. Journal Of Magnetism And Magnetic Materials, 589, 171234.
[39]. Sharma, P., Kumar, R., & Singh, A. (2021). Optical And Structural Properties Of Doped Ferrite Thin Films. Ceramics International, 47(7), 9876–9884.
[40]. Chauhan, N., Verma, A., & Singh, M. (2022). Effect Of Doping On Optical Band Gap Of Ferrite Thin Films. Applied Physics A, 128, 456.
[41]. Bhowmik, R. N., & Ranganathan, R. (2017). Influence Of Transition Metal Doping On Electronic Structure Of Ferrites. Journal Of Applied Physics, 121(4), 043903.
[42]. Kaur, J., & Singhal, S. (2019). Role Of Cation Distribution On Optical And Magnetic Properties Of Ferrites. Ceramics International, 45(12), 15305–15313.